Bond Tests Under High Loading Rates

Mathias Michal[(⊠)] and Manfred Keuser

Universität der Bundeswehr München, Werner-Heisenberg-Weg 39,
85577 Neubiberg, Germany
{mathias.michal, Manfred.keuser}@unibw.de

Abstract. The bond behavior between steel and concrete under high loading rates has been investigated. Different test configurations have been developed and an extensive test program has been performed. The results served as a basis for the development of a model for the bond behavior, where the influence of high strain rates is considered. Similar to the mechanical properties of concrete and steel also their interaction changes with an increase of the loading rate. The low rate dependency of steel compared to concrete with the simultaneous increase of the ultimate bond-stress can lead to a more brittle structural behavior. The knowledge of the rate dependent bond behavior is the condition for the nonlinear analyses of high-dynamic stressed reinforced structural components, if system reserves should be activated by the formation of plastic hinges, a sealing effect against fluids and gases has to be ensured and the crack width or the deformation should be limited. To cover a broad range of loading rates, the experiments have been performed on different test facilities. While the tests with loading velocities up to 1 m/s could be performed on hydraulic systems, for loading rates up to 17 m/s a test configuration with a split-hopkinson-bar has been developed. With this experimental technologies bond tests with slip rates in the range of $9.2 \cdot 10^{-6}$ m/s to 0.9 m/s, respectively bond stress rates from 0.22 MPa/s to $2.1 \cdot 10^{5}$ MPa/s have been realized. About 183 Push-In tests with cylindrical test specimens and short bond lengths have been carried out. The concrete compressive strength, the diameter of the specimen, the diameter of the bar, the surface of the reinforcement and the bond length have been varied.

Keywords: Bond model · High strain rates · Split-Hopkinson-Bar (SHB)

1 Introduction

The rate dependency of bond between steel and concrete has been investigated by different researchers in the past [e.g. Hjorth 1976, Vos 1983, Solomos and Berra 2010]. Hydraulic devices, Split-Hopkinson-Bars and Drop-Towers have been used therefor. Similar to the mechanical properties of concrete and steel also their interaction changes with an increase of the loading rate. Based on a literature review a comprehensive description of the main results of research about rate dependent bond behavior is given in Michal and Keuser (2014).

It is well known that concrete shows, after a moderate increase up to a strain rate of $\dot{\varepsilon} \approx 10^{1} s^{-1}$, a significant increase of strength for higher strain rates. For strain rates about $10^{6} \ s^{-1}$ the concrete compressive strength more than doubles and the concrete

tensile strength increases up to six times the quasistatic strength [Curbach and Quast 2014]. Possible causes are the moisture content due to the Stéfan-Effect, inertial effects connected to the crack propagation or an increase of crack formation. Their weightings are still contentious.

To investigate the bond behavior between steel and concrete under high loading rates, suitable experimental methods have been developed and an extensive amount of bond tests have been performed. On basis of these experimental results a bond model to describe rib-shear failure and splitting failure under consideration of the loading rate was suggested.

2   Experimental Investigation.

Materials. Within the experimental study the concrete compressive strength (f_{cm} = 15 MPa to 87 MPa), the diameter of the specimen (D_c = 70 mm and 105 mm), the diameter of the bar (d_s = 10 mm and 14 mm), the surface of the reinforcement (P = indented steel, R = ribbed steel), the bond length (l_b = 30 mm to 100 mm) and the loading rate were varied. The combination of parameters for all tests is shown in the table in Fig. 1. There have been two main series, s1 with indented steel and s2 with ribbed steel, where only the concrete compressive strength has been changed. Natural aggregates with aggregate sizes of 0/4 and 4/8 and cement CEM I of the strengths 32.5 R, 42.5 R and 52.5 R have been used. The mean concrete compressive strength was determined on cubes with an edge length of 150 mm.
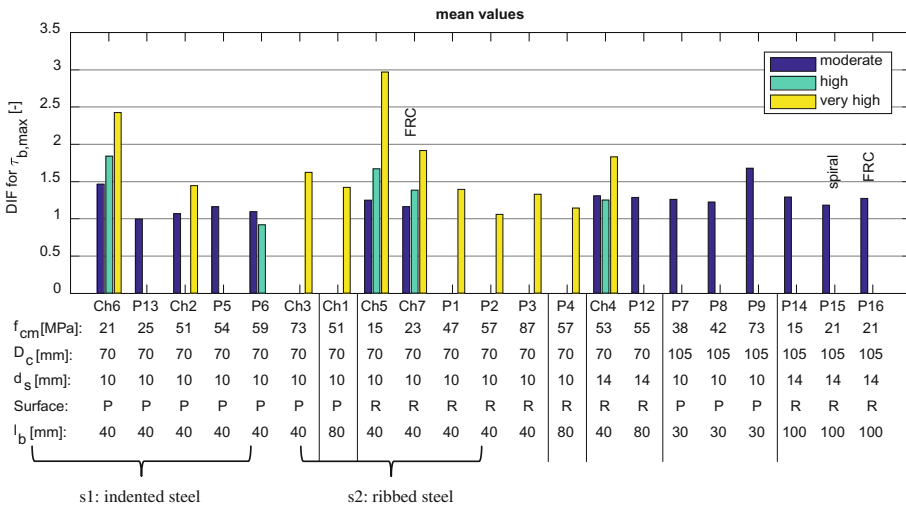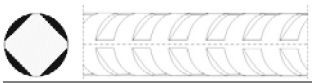

Fig. 1. DIF for the maximum bond strength

Two types of steel have been used, indented steel (P) and ribbed steel (R) according to DIN EN 10080. Their geometric specifications, diameter of the bar **d**, indentation depth in the center or rib height at the mid-point $\mathbf{a_m}$, transverse rib or indentation spacing **c**, average gap between two adjacent rib or indentation rows **e** are shown in Table 1 for the indented steel and in Table 2 for the ribbed steel. The relative indentation area f_P and the relative rib area have been calculated with the parabola formula according to DIN ISO 15630. The characteristic yield strength of 500 MPa wasn´t reached in the tests due to the short bond lengths.

Table 1. Surface geometry of the indented steel (P).

	d	a_m	c	e	f_P
	10,4 mm	0,5 mm	5,7 mm	2,6 mm	0,040

Table 2. Surface geometry of the ribbed steel (R).

	d	a_m	c	e	f_R
	9,5 mm	0,6 mm	6,1 mm	1,9 mm	0,060

Methods. To cover a broad range of loading rates, the experiments have been performed on different test facilities. While the tests with a rate of slip increase up to 1 m/s could be performed with hydraulic systems, for rates up to 17 m/s a test configuration with a Split-Hopkinson-Bar has been developed. The Split-Hopkinson-Bar (SHB) is often used to determine the uniaxial material properties for medium strain rates [Curbach and Quast 2014]. Thereby the specimen is sandwiched between an incident and an output bar. With a loading device a stress wave is induced in the incident bar. At the interface between bar and specimen the wave is partly reflected and partly transmitted to the specimen. This process is repeated at the transition to the output bar and leads to multiple reflection in the specimen. If the time, the wave needs to pass through the specimen is essential short compared to its temporal extension, a uniform stress and strain distribution is assumed and the well known formulae for the analysis of the SHB-Test based on the propagation of a one-dimensional wave can be used. For the bond tests the push-in specimen was installed between an incident bar of 5 m length and the output bar 3.5 m length. To introduce the load to the reinforcement bar and to measure the slip of the reinforcement two transition cylinders have been added to the bars (Fig. 2). The bars and the transition cylinders have had a diameter of 75 mm and were made of aluminium.

With specially drilled holes and a mirror it was possible to measure the translation of the bar with a vibrometer. The slip was determined by the difference of the signal given by the vibrometer and the overall displacement of the specimen calculated from
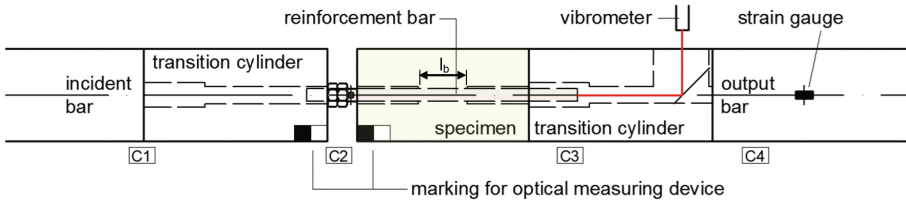
Fig. 2. Schematic push-in test configuration

the time-shifted signal of the strain gauge mounted on the output bar. The mathematical algorithms used are described in Michal et al. (2015).

Similar to the tests with very high velocity on the SHB also in the tests with the hydraulic devices the bar was pushed into the specimen. While for the quasistatic and tests with moderate velocity the rebar was connected directly to the loading device, for the tests with high velocity the reinforcement was hammered by a hydraulically accelerated ram into the concrete specimen.

The loading rate has been classified according to the bond stress respectively bond slip rate obtained within the test (Table 3).

**Table 3.** Speed range with bond stress and slip rate.

Loading rate LR	Bond stress rate $\dot{\tau}$ [MPa/s]			Slip rate $\dot{s}$ [m/s]		
	Range	Mean	V* [%]	Range	Mean	V* [%]
Quasi-static	0.044–0.41	0.22	45	$4.0 \cdot 10^{-6}$–$1.7 \cdot 10^{-5}$	$9.2 \cdot 10^{-6}$	42
Moderate	22–100	69	36	$1.1 \cdot 10^{-3}$–$7.2 \cdot 10^{-3}$	$4.0 \cdot 10^{-3}$	44
High	$7.5 \cdot 10^{3}$–$1.8 \cdot 10^{4}$	$1.3 \cdot 10^{4}$	34	0.36–0.83	0.54	48
Very high	$1.3 \cdot 10^{5}$–$3.7 \cdot 10^{5}$	$2.1 \cdot 10^{5}$	39	5.3–17.0	9.9	42

*variance

3   Results

Quasistatic Bond Tests. The concrete compressive strength was varied in a range of f_{cm} = 15 MPa to 85 MPa. Figure 3a shows the *maximum bond strength* for ribbed and indented steel over the concrete compressive strength.

Figure 3 shows also the predictions according to MC2010 for "good bond conditions" and "all other bond conditions". When considering the scatter in bond tests, the results agree well with the calculated curves. For both surfaces the maximum bond strength increased for increasing concrete compressive strength. The maximum bond strength achieved by the ribbed steel was about 25% to 48% higher than for indented steel. This difference grew larger with increasing concrete strength. The *to the maximum bond strength associated slip* s_0 was about 1.1 mm for indented steel. For the ribbed steel the slip was decreasing with increasing concrete compressive strength (Fig. 3b). While the *bond stiffness* was proportional to the concrete compressive
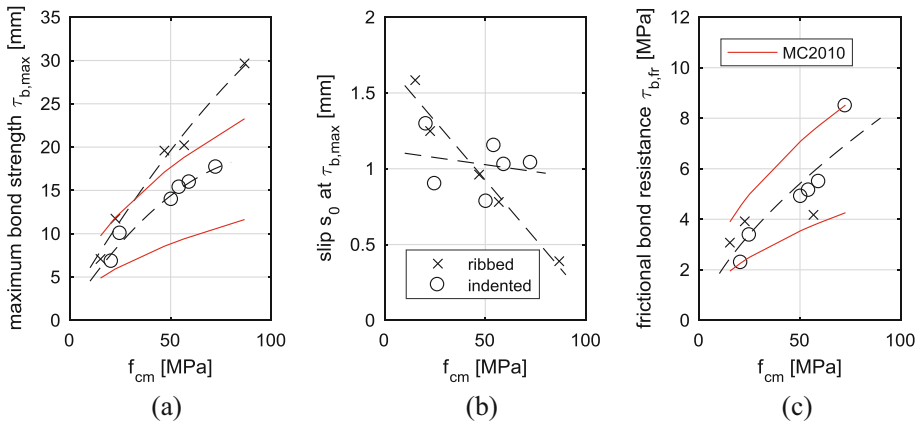
Fig. 3. Maximum bond strength (a), associated slip (b) and frictional bond resistance (c) for ribbed and indented steel in the quasistatic experiments

strength for indented steel, it showed a significant increase for ribbed steel from a concrete compressive strength higher than $f_{cm} = 40$ MPa. For the *frictional bond resistance* no significant differences could be observed for the two used types of rebars (Fig. 3c). After shearing off the compacted concrete between the ribs respectively the profiling a comparable sliding surface forms between the bar and the concrete. There is still an interdependence between the frictional resistance and the concrete compressive strength.

The upper limit for the bond resistance is given with a bond stress – slip relationship that defines the characteristic maximum bond strength $\tau_{b,max}$, the frictional bond resistance $\tau_{b,fr}$ and the corresponding values for the slip. Tepfers (1973) used the model of a thick walled cylinder to describe splitting failure. This approach formed the basis for further models proposed by other researchers [e.g. Vandewalle 1992]. It's important to consider, that all of these models are strongly dependent of the inclination of the concrete struts. With increasing slip also the angle of spread changes for the compressive stresses and therefore also the resulting tensile stresses around the bar. By taking this into consideration one can define the border lines for the slip dependent bond stress and the slip dependent maximum bond stress determined by splitting failure. Basically three different cases can be distinguished.

For confined concrete the transferable bond stress is determined by the shear resistance of the concrete struts between the ribs. The bar is pulled out of the concrete (Fig. 4a). For concrete cover smaller then about 3 to 4 times the bar diameter crack formation longitudinal to the bar will lead to a brittle failure when a bond stress equal to the intersection of the bond stress – slip relationship with the borderline for the maximum bond stress for splitting is reached (Fig. 4c). There is also an undetermined area, where as well shearing of the concrete between the ribs as splitting of the concrete cover can be the leading failure mechanism (Fig. 4b). Also a combined failure of shear and splitting can occur. While for quasistatic tests after exceeding the maximum bond stress for pull-out splitting wasn't relevant any more, for the dynamic tests a delayed
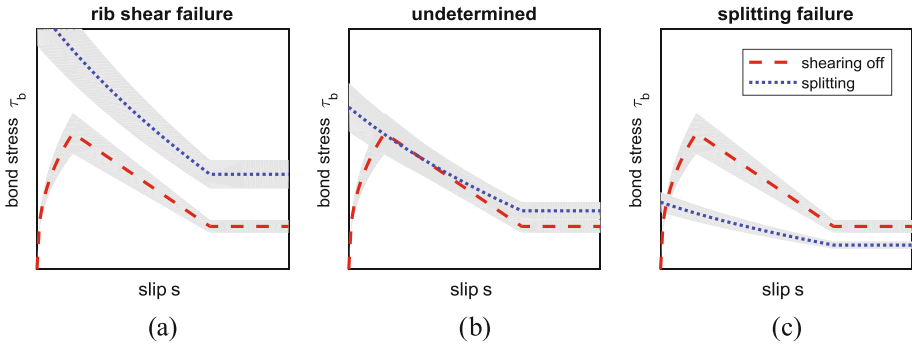
Fig. 4. Border lines for $\tau_b(s)$ at shear failure and for $\tau_{b,max}(s)$ at splitting failure

splitting in the decreasing part of the bond stress – slip relationship was observed for some specimens.

Dynamic Bond Tests. In addition to the quasistatic tests experiments with moderate, high and very high velocity have been conducted. When the maximum bond stress $\tau_{b,max}$ is divided by the mean $\tau_{b,max}$, obtained in the quasistatic tests, the quotient is the dynamic increase factor (DIF). The tests cover a wide range for the bond stress rate and showed a good correspondence to results given in literature. Figure 5 shows the DIF for the maximum bond strength in dependence of the bond stress rate for all tests and the results obtained by Hjorth (1976) and Vos (1983). With increasing bond stress rate an increase of the DIF can be recognized but also a large variation of the values.
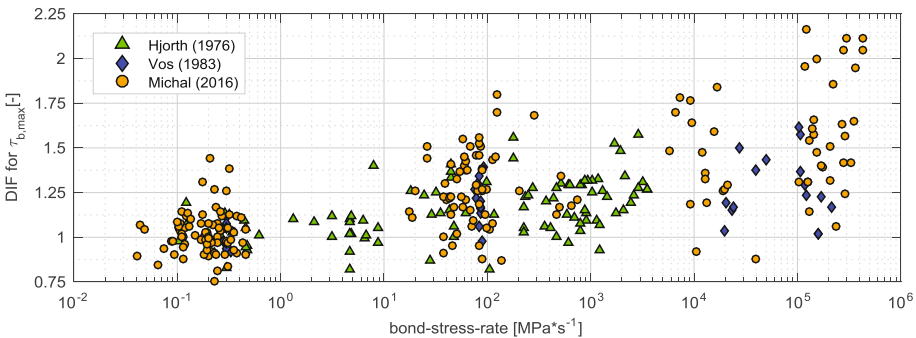
Fig. 5. DIF for the maximum bond strength, test results compared to literature

Figure 1 shows the DIF for the maximum bond strength separated for the different test batches. While the DIF increases with increasing velocity it decreases for higher concrete strengths. Another reason for the scatter of the DIF is a change of the failure mechanism. Specimens, failing by shearing off the concrete between the ribs in the

quasistatic tests failed by splitting of the concrete cover in the high velocity tests. This was mainly observed for the specimens with the ribbed bars.

The reason for the increase of the bond strength seems to be the rate dependency of the concrete. The formulae proposed for the consideration of the loading velocity are based on the following assumptions:

- For high loading velocity the same failure mechanisms occur as for quasistatic loading.
- There is no influence of the loading rate on the angle under which the bond forces spread into the concrete.
- Shear and splitting failure can be considered separately.

Bond stress transfer is always connected to a relative displacement between steel and concrete and the formation of cracks. Already after a slight displacement the Chemical Adhesion is overcome and the main mechanism of bond, the mechanical interlock is activated. Thereby the ribs of the bar are bracing concrete consoles in the concrete surrounding the steel. Primary cracks initiate from the ribs. For pull-out failure, the concrete consoles between the ribs are shearing off and only the frictional resistance remains for the transmission of forces (Fig. 6a). The spatial stress condition in the concrete leads to circular tensile forces that can result in splitting of the concrete cover (Fig. 6b).

(a)   (b)

Fig. 6. Principal stresses at the failure surface for shear failure(a) and around the bar for splitting failure (b)

For shear failure the strain rate in the concrete depends on the deformation of the concrete struts between the ribs and thereby on the slip and the surface of the steel. For plain steel an identical slip rate leads to a lower strain rate compared to deformed steel. Moreover for deformed steel the slip leads to a radial displacement of the concrete ring

that is connected to the struts. Due to inertia a dynamic confinement creates additional friction. To consider the influence of the loading velocity the relative strain rate $\dot{\varepsilon}_{PO}^* = \dot{s}/L^*$ is proposed. The Length L^* was chosen as the distance of the ribs respectively the indentation. With $\dot{\varepsilon}_{PO}^*$ the DIF for the concrete compressive strength and with $\dot{\varepsilon}_{SP}^* = \varepsilon_{ct,max,stat} \cdot \dot{\tau}_b/\tau_{b,max}$, where $\varepsilon_{ct,max,stat}$ is the ultimate strain for concrete in tension, $\dot{\tau}_b$ is the bond stress rate and $\tau_{b,max}$ is the maximum bond stress, the DIF for the concrete tensile strength were calculated using the formulas given in CEB Bulletin 187 (1988). Thereafter the dynamic bond strength can be calculated using the same formulae given for quasistatic bond behavior.

In Fig. 7 the experimental results obtained in charge 2 (f_{cm} = 51 MPa, d_s = 10 mm (P), l_b = 40 mm) are given together with the analytical results for quasistatic, moderate and very high loading rates. In the quasistatic tests the bond failed by shearing off the concrete between the ribs. With increasing loading rate also the bond resistance increased. It is important to consider, that the observed dynamic increase is influenced not only by the loading rate but also by the failure mechanism.
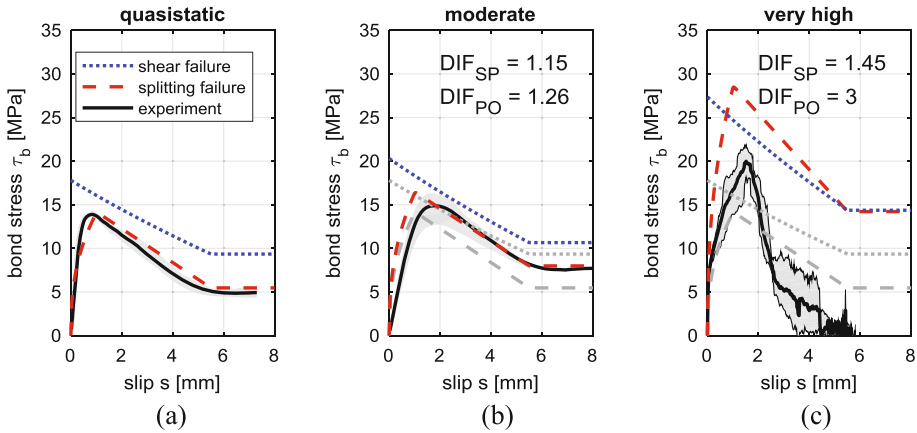

Fig. 7. Charge 2: f_{cm} = 51 MPa, d_s = 10 mm (P), l_b = 40 mm

While the increase of the bond shear resistance is determined by the strain rate of the concrete between the ribs, the increase of the splitting resistance depends on the strain rate of the concrete around the bar (Fig. 6).

4   Conclusion

With the conducted Push-In tests the basis was laid for the formulation of a rate dependent bond stress-slip relationship that can be used in numerical simulations. The ultimate bond stress and the whole bond stress-slip relationship have been obtained in the tests. The investigation of dynamic material properties is a great challenge. The requirements on the test equipment are more complex compared to quasistatic tests. Inertial effects, the

component geometry and the characteristic of wave propagation have to be considered. The configuration for the dynamic Push-In bond tests is based on a Split-Hopkinson-Bar. The Split-Hopkinson-Bar is established for the dynamic material characterization and was therefore also used in this research project. However, different parameters of bond behavior which are deemed relevant by the authors can´t be investigated due to limitations of this configuration. For the interpretation of test results it is important to consider the geometry of the specimens. To reduce the influence of an arching effect on bond shear failure due to friction between the specimen and the support area a bond free length has been chosen. This leads to an increased splitting resistance, because of the additional area for the absorbtion of tensile hoop stresses. To model the bond behavior as well for quasistatic as for high-dynamic loading the bond-shear- and bond-splitting-failure has to be analysed separately. The maximum bond strength is obtained by the superposition of the boundary lines of both failure mechanisms. With the chosen model a good agreement to the experimental results was achieved. The results of this investigation indicate, that the reason for the changes in bond behavior under high loading rates are based on the rate dependent concrete strength.

References

Comite Euro-International du Beton, CEB: Concrete Structures under Impact and Impulsive Loading, Bulletin d'Information No. 187, Lausanne (1988)

Comite Euro-International du Beton, CEB: Bond of reinforcement in concrete, State-of-art report, Bulletin 10, Lausanne (2000)

Curbach, M., Quast, M.: Concrete under biaxial impact loading. In: Hopkinson Cenetary Conference Cambridge, UK, pp. 117–135 (2014)

Hjorth, O.: Ein Beitrag zur Frage der Festigkeiten und des Verbundverhaltens von Stahl und beton bei hohen Dehnungsgeschwindigkeiten, Dissertation, TU Braunschweig (1976)

Michal, M., Keuser, M.: Bond of steel and concrete under high loading rates. In: Proceedings of the 9th International Conference on Structural Dynamics, EURODYN 2014, Porto, Portugal, 30 June–2 July 2014, pp. 3491–3495 (2014)

Michal, M., Keuser, M., Solomos, G., Peroni, M., Larcher, M., Esteban, B.: Experimental investigation of bond strength under high loading rates. In: Proceedings of the 11th DYMAT, Lugano, Switzerland, 7–11 September 2015, pp. 01044-1–01044-5 (2015)

Solomos, G., Berra, M.: Rebar pullout testing under dynamic Hopkinson bar induced impulsive loading. Mater. Struct. **43**, 247–260 (2010)

Tepfers, R.: A Theory of Bond Applied to Overlapped Tensile Reinforcement Splices for Deformed Bars, Pub. 73:2, Chalmers University of Technology, Göteborg (1973)

Vandewalle, L.: Theoretical prediction of the ultimate bond strength between a reinforcement bar and concrete. In: Proceedings of the International Conference on Bond in Concrete, Riga, Latvia, 15–17 October 1992, pp. 1.1–1.8 (1992)

Vos, E.: Influence of loading rate and radial pressure on bond in reinforced concrete, Ph.D. thesis, Delft University of Technology (1983)